

~~CONFIDENTIAL~~203  
Copy  
RM L53G23a

NACA RM L53G23a

~~52-36-14~~

NACA

D144389

TECH LIBRARY KAFB, NM

## RESEARCH MEMORANDUM

TS41

THE EFFECT OF CONTROL-SURFACE-SERVO NATURAL FREQUENCY ON  
THE DYNAMIC PERFORMANCE CHARACTERISTICS OF AN  
ACCELERATION CONTROL SYSTEM APPLIED TO A  
SUPERSONIC MISSILE

By Anthony L. Passera and Martin L. Nason

Langley Aeronautical Laboratory  
Langley Field, Va.

CLASSIFIED DOCUMENT

This material contains information affecting the National Defense of the United States within the meaning  
of the espionage laws, Title 18, U.S.C., Secs. 793 and 794, the transmission or revelation of which in any  
manner to unauthorized persons is prohibited by law.

NATIONAL ADVISORY COMMITTEE  
FOR AERONAUTICS

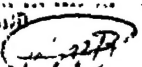
WASHINGTON

September 29, 1953

~~CONFIDENTIAL~~*HANCOCK*

Classification cancelled (or changed) ~~Declassified~~

By Authority of NASA Technical Document Control  
~~05/17/74 S3 TO CHANGE~~

By..... NAME AND 

GRADE OF OFFICER MAKING CHANGE)

... 10 General  
DATE

1R

NACA RM L53G23a

~~CONFIDENTIAL~~

TECH LIBRARY KAFB, NM



0144386

NATIONAL ADVISORY COMMITTEE FOR AERONAUTICS

RESEARCH MEMORANDUM

THE EFFECT OF CONTROL-SURFACE-SERVO NATURAL FREQUENCY ON  
THE DYNAMIC PERFORMANCE CHARACTERISTICS OF AN  
ACCELERATION CONTROL SYSTEM APPLIED TO A  
SUPERSONIC MISSILE

By Anthony L. Passera and Martin L. Nason

SUMMARY

A theoretical investigation was conducted to determine the effects of control-surface-servo natural frequency on the dynamic performance characteristics of a supersonic canard missile configuration stabilized longitudinally by controlling the normal acceleration of the missile.

The analysis indicated that some improvement in control-system accuracy was obtained by using a high natural frequency control-surface servo; however, the additional cost and the higher rate of oil flow might prohibit designing a control-surface servo with a natural frequency greater than 70 or 80 radians per second in view of the small additional improvement in control accuracy obtained.

With smaller sized geometrically similar missiles, greater accuracy of control was achieved, smaller volume of oil was necessary, and a decrease in the peak rate of oil flow was realized.

INTRODUCTION

The general research program of automatic control and stabilization at the Pilotless Aircraft Research Division of the Langley Aeronautical Laboratory is concerned with the dynamic performance characteristics of an automatically controlled supersonic missile configuration. The types of automatic control systems presently under study are pitch attitude, flight path, normal acceleration, and roll. One or a combination of these control systems might be used with a guidance system to control the motion of a missile.

~~CONFIDENTIAL~~

1

*[Handwritten signature]*

~~CONFIDENTIAL~~

NACA RM L53G23a

A study for this missile configuration was made on the attitude control system and is presented in references 1 and 2. The conclusions reached in these references were that a small static-margin airframe with rate-of-pitch feedback yielded satisfactory system performance and that only small improvements in attitude control accuracy for servo natural frequencies greater than 70 or 80 radians per second resulted. Since both the volume of oil and the peak rate of oil flow for the servo increased with servo natural frequency for the attitude control, these factors may prohibit designing an autopilot with a natural frequency greater than 70 or 80 radians per second in view of the small improvements in system response. The cost of construction associated with high-performance servos is another factor limiting servo natural frequency.

The automatic-control system considered in this report is sensitive to normal acceleration. The analysis includes the effects of both servo natural frequency and missile size over a range of flight conditions. In reference 3, it was concluded that for an acceleration control system more rapid responses could be obtained with larger static margins (distance between missile aerodynamic center and center of gravity); consequently, the stability derivatives corresponding to the large-static-margin case (0.564 mean aerodynamic chord) are used throughout this analysis. With this static margin, normal-acceleration and control-surface-deflection transient responses were obtained at various flight conditions for a range of servo natural frequencies and missile sizes. The transient responses and summary plots made from them are presented in this paper.

## SYMBOLS

$\bar{c}$	mean aerodynamic chord, 1.776 feet
$g$	acceleration due to gravity, $32.2 \text{ ft/sec}^2$
$K_A$	static gain constant of control-surface-servo transfer function ( $\delta/V$ ), deg/volt
$K_g$	static gain constant of airframe transfer function $n_o/\dot{\theta}$ , g units/deg/sec
$K_m$	static gain constant of airframe transfer function $\dot{\theta}/\delta$ , deg/sec/deg
$K_r$	proportionality constant between rate-feedback voltage $V_1$ and the missile rate of pitch $\dot{\theta}$ , volts/deg/sec

~~CONFIDENTIAL~~

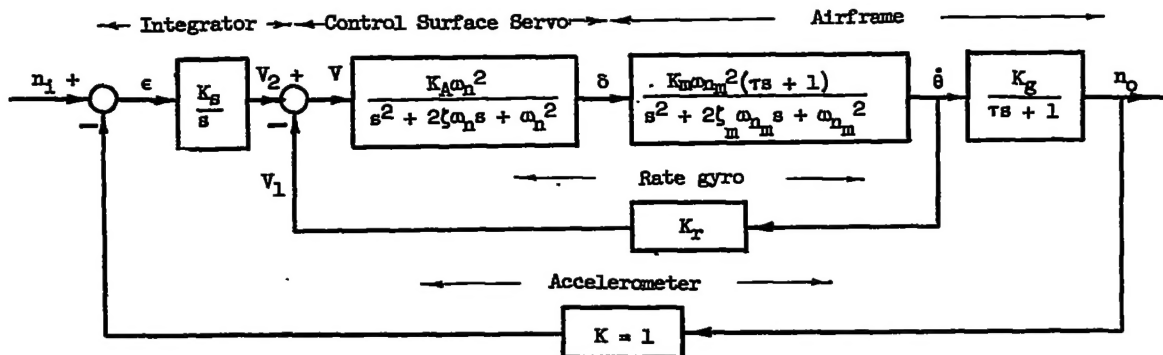
$K_s$	proportionality constant between integrator output $\dot{V}_2$ and control-system error signal $\epsilon$ , volts/sec/g unit
$M$	Mach number
$n_1$	control-system acceleration input signal, g units
$n_0$	control-system acceleration output signal, g units
$s$	Laplace transform variable
S.F.	size factor, ratio of characteristic length of a missile geometrically similar to prototype to a characteristic length of prototype
$V$	inner-loop error signal, $V_2 - V_1$ , volts
$\epsilon$	acceleration error signal of control system, $n_1 - n_0$ , g units
$\delta$	pitch canard control-surface deflection, deg
$\zeta$	quadratic damping ratio of control-surface servo, nondimensionalized constant
$\zeta_m$	quadratic damping ratio of airframe, nondimensionalized constant
$\theta$	pitch angle of airframe, deg
$\tau$	time constant of airframe linear factor, sec
$\omega_n$	undamped natural frequency of control-surface servo, radians/sec
$\omega_{n_m}$	undamped natural frequency of airframe, radians/sec
$\int  \epsilon(t)  dt$	control-system accuracy, g-sec

A dot over a symbol denotes a derivative with respect to time.

#### DESCRIPTION OF THE CONTROL SYSTEM

The acceleration control system considered in this paper consists of a supersonic missile, a control-surface servo, an ideal integrator,

an ideal accelerometer, and an ideal rate gyro.



The following is a description of the control-system block diagram shown above. An input command signal  $n_1$  calls for a change in normal acceleration. The error signal that causes the system to respond is

$$\epsilon(s) = n_1(s) - n_0(s)$$

where the feedback signal  $n_0(s)$  is furnished by an ideal accelerometer. The integrator responds to this signal and produces an output  $V_2$  that satisfies the transfer function

$$\frac{V_2(s)}{\epsilon} = \frac{K_s}{s}$$

An integrator was necessary in the control system since a zero steady-state acceleration error was desired.

The rate gyro produces a signal  $V_1$  that is proportional to  $\dot{\theta}$ . This unit supplies additional damping to and improves the speed of response of the control system.

The control-surface servo responds to the difference of these two signals

$$v(s) = v_2(s) - v_1(s)$$

and causes the control-surface servo to respond in accordance with the transfer function

$$\frac{\delta(s)}{v} = \frac{K_A \omega_n^2}{s^2 + 2\zeta \omega_n s + \omega_n^2}$$

In the analysis four control-surface servos were considered with the following coefficients:  $\omega_n = 30, 50, 80$ , and  $150$  radians per second;  $\zeta = 0.5$ . A possible arrangement for a control-surface servo having such a second-order characteristic equation is illustrated in figure 1.

The missile considered in this paper is a symmetrical cruciform configuration shown in figure 2, and this missile is the prototype or missile referred to as having a size factor of unity. The wings and canard fins are of delta design with leading edges swept back  $60^\circ$  and have modified double-wedge cross sections. Required longitudinal control is provided by the horizontal canard fins. The missile transfer functions based upon the conventional two-degree-of-freedom longitudinal equations of motion are:

$$\frac{\dot{\theta}(s)}{\delta} = \frac{K_m \omega_{n_m}^2 (\tau s + 1)}{s^2 + 2\zeta_m \omega_{n_m} s + \omega_{n_m}^2}$$

$$\frac{n_o(s)}{\theta} = \frac{K_g}{\tau s + 1}$$

The values of the above airframe constants are given in table I and are based upon a flight test of the missile reported in reference 4.

## ANALYSIS AND DESIGN PROCEDURE

The purpose of this investigation is to determine the effect of control-surface-servo natural frequency over a range of Mach numbers, altitudes, and missile sizes. A brief summary of the analytical and graphical methods of analysis employed in this investigation follows.

## Gain Adjustment Criteria

In the synthesis of a control system, the customary procedure is to design the system with certain specific objectives in mind. These objectives, which are dictated by the particular application or job the system is required to perform, often impose certain restrictions on the transient performance characteristics. In this particular analysis the system gains were adjusted to yield a near-minimum value for  $\int |\epsilon(t)| dt$ . Actual adjustment of the gains  $K_r$  and  $K_s$  was done graphically by methods outlined in reference 5. In most instances, it was found necessary to achieve approximately an amplitude ratio of unity for  $\frac{n_o(j\omega)}{n_i}$  over a wide frequency range to make  $\int |\epsilon(t)| dt$  approach a minimum value. Reference to a system with high accuracy of control is considered equivalent to a system with a small value of  $\int |\epsilon(t)| dt$  throughout this paper.

Examples of the control-system frequency responses are illustrated on figure 3. These responses are plotted on Nichols charts (see ref. 6, p. 319) for a size factor of unity at  $M = 1.6$  for sea-level conditions. Only four charts are shown in figure 3 since they are representative of the other size factors.

Adjustment of the system gains was conducted for  $M = 1.6$  at sea level for various servo natural frequencies and size factors. The system operation was also investigated at other flight conditions for a size factor of unity by utilizing the gains obtained for  $M = 1.6$  at sea level.

The conditions under which the gains were adjusted are summarized in the following table.

Size factor	Natural frequency, radians/sec	Flight condition	Gain adjustment
0.4	30, 50, 80, 150	M = 1.6; sea level	Gain adjusted at each $\omega_n$
.7	30, 50, 80, 150	M = 1.6; sea level	Gain adjusted at each $\omega_n$
1.0	30, 50, 80, 150	M = 1.6; sea level	Gain adjusted at each $\omega_n$
2.0	30, 50, 80, 150	M = 1.6; sea level	Gain adjusted at each $\omega_n$
1.0	30, 50, 80, 150	M = 1.2; sea level	Same gains as M = 1.6 and at sea level
1.0	30, 50, 80, 150	M = 1.6; 40,000 ft	Same gains as M = 1.6 and at sea level
1.0	30, 50, 80, 150	M = 2.0; sea level	Same gains as M = 1.6 and at sea level

The gains  $K_r$  and  $K_s$  determined in the analysis are given in table II. For convenience, the static gain  $K_A$  was arbitrarily chosen as unity throughout the analysis; however, this choice was not necessary since it always appeared in combination with  $K_r$  and  $K_s$ . Consequently, these three gains,  $K_A$ ,  $K_r$ , and  $K_s$  may be modified appropriately to give the same products  $K_A K_r$  and  $K_A K_s$  obtained in the analysis.

The transient responses were determined by the Laplace transform method. Roots of the characteristic equation are given in table III.

#### Size Effect

In determining the size of a missile configuration, consideration must be given to its application, and very often the size of the components for the control as well as the guidance system dictate the size of the missile. Since the missile size may vary with the application and the selection of components, an investigation of the effect of missile size on the system response was included.

~~CONFIDENTIAL~~

NACA RM L53G23a

Variations in model dimensions affect the basic transfer function of the airframe. By assuming that the stability derivatives are functions of Mach number alone, that the density of the over-all missile is independent of the size, and that the mass distribution is the same, it can be shown that the constants given in table I are valid. These assumptions are believed to be realistic for the range of size factors considered herein.

#### Volume and Peak Rate of Oil Flow

The volume of oil and peak rate of oil flow through the servo are significant factors when viewed from an economic standpoint. Systems requiring the smallest amount of stored oil and the lowest peak rate of flow while not violating other system requirements are the most desirable. If it is assumed that the control-surface deflection is proportional to the servomotor displacement and that the piston area is constant for all size factors, flight conditions, and servo natural frequencies, then the total volume of oil consumed and the peak rate of flow is proportional to  $\int |d\delta|$  and  $\dot{\delta}_{max}$ , respectively.

#### RESULTS AND DISCUSSION

The purpose of this paper is to study the effect of servo natural frequency on the dynamic performance characteristics of an acceleration control system over a range of size factors, Mach numbers, and altitudes.

The calculated missile normal acceleration  $n_0$  and control surface angular deflection  $\delta$  transient responses to a unit step acceleration input  $n_1$  are plotted in figures 4 and 5 for the various size factors, flight conditions and servo natural frequencies. Evaluation of the system is conducted essentially on two separate topics: (1) normal-acceleration transient-response characteristics and (2) control-surface-servo characteristics. The former is broken down into  $\int |\epsilon(t)| dt$ , rise time, and response time defined graphically in figure 6 and the latter into  $\int |d\delta|$  and  $\dot{\delta}_{max}$  discussed previously. Rise and response times were found by direct examination of the normal-acceleration time histories. The time integral of the magnitude of the acceleration error was measured with a planimeter and the integration was taken between zero time and the time when the output reaches and remains within

~~CONFIDENTIAL~~

5 percent of the steady-state value. Total control-surface angular deflection  $\int |\delta| dt$  was obtained from the  $\delta$  transients, and the maximum time rate of change of control-surface deflection  $\dot{\delta}_{\max}$  from the  $\dot{\delta}$  transients. The above-mentioned characteristics of the control system have been plotted against servo natural frequency in figures 7 and 8.

#### Transient Performance Characteristics

Examination of the  $\int |\epsilon(t)| dt$  shown on figure 7 indicates that,

for a size factor of 2.0, no appreciable increase in control accuracy is obtained by increasing the control-surface-servo natural frequency beyond 80 radians per second. For smaller size factors, however, the value of servo natural frequency beyond which the increased accuracy of control becomes insignificant is slightly higher than 80 radians per second. Apparently, this effect is caused by the increased missile natural frequency associated with smaller size factors (see table I); thus, the airframe is allowed to respond to a greater range of frequencies.

Mach number and altitude effects on the transient performance characteristics may be ascertained by further examination of figure 7. Increasing the Mach number from 1.2 to 2.0 yields only a slight system improvement, whereas increasing the altitude from sea level to 40,000 feet decreases the accuracy of control by a factor of approximately 3.

Figure 7 also illustrates the manner in which the transient characteristics are affected by size factor. The system with the smallest size factor has the smallest  $\int |\epsilon(t)| dt$  so that an advantage in keeping the missile small is indicated; however, the lower limit on size may be determined by the space needs of the servomotor and associated gear, seeker equipment, rocket propellant, and warhead. Since it can be shown that the normal acceleration due to aerodynamic causes is inversely proportional to the size factor, this higher accuracy associated with the smaller missiles seems reasonable. For this control system, an almost linear relationship between the accuracy of control and size factor for all servo natural frequencies is obtained.

The gain adjustments were made to obtain nearly minimum error control and thus whatever rise time and response time resulted were accepted. Note in figure 7, however, that these three transient characteristics

$\int |\epsilon(t)| dt$ , rise time, and response time, in general, all follow the

same trend as various system parameters are allowed to change. Thus, these three quantities are somewhat interdependent.

#### Control-Surface-Servo Characteristics

The manner in which  $\dot{\delta}_{\max}$  and  $\int |\delta| dt$  vary with servo natural for the size factors and flight conditions studied is shown in graphical form in figure 8. It will be noticed that the peak rate of flow increases with servo natural frequency for all size factors and flight conditions.

Further examination of figure 8 indicates that a slight saving in the total oil flow or accumulator volume may be made by using the higher natural-frequency servos for all size factors, the reason being the improved damping of the control-system transient responses which accompanies the increased natural frequency of the servo. This improved damping may be confirmed by either direct examination of the  $n_0$  and  $\delta$  transient responses or by noting the relative magnitude of the real parts of the complex roots of the characteristic equation defining the oscillatory modes of motion given in table III. Hence, slightly smaller accumulators can be used with control-surface servos characterized by higher natural frequencies.

Figure 8 shows the effects of Mach number and altitude on the servo characteristics. The total volume of oil and the peak rate of oil flow requirements decrease with increasing Mach number, but this saving is so small as to be nearly negligible compared with other effects. Altitude effects may be ascertained by comparison of the plots for  $M = 1.6$ . A change of 40,000 feet in altitude will require 4 to 5 times as much oil flow and a slightly higher peak rate of oil flow for a change in normal acceleration of 1 g.

Figure 8 also shows size-factor effects. The peak rate of flow increases substantially with size factor for all servo natural frequencies. The total volume of oil flow is approximately a linear function of the size factor. These two figures imply that a decrease in both total volume of oil flow and peak rate of flow would be realized for a smaller missile configuration stabilized in an acceleration control system.

#### Choice of Servo Natural Frequency

The preceding sections now give a sufficient amount of information with which to discuss the problem of choosing a desirable servo natural frequency for this control system. Since the  $\int |\epsilon(t)| dt$  decreases while the peak rate of flow and cost of construction increases as the servo

natural frequency increases, some sort of compromise between these system characteristics must be obtained. If high accuracy of control is mandatory, a sacrifice in cost and peak rate of volume flow must be made and, conversely, if a low degree of accuracy is tolerable, relatively inexpensive low-frequency servos will be adequate.

Figures 7 and 8 illustrate that 80 radians per second may be a good compromise value of control-surface-servo natural frequency for the flight conditions and size factors considered. Beyond 80 radians per second, the accuracy of control does not improve sufficiently to offset the increased cost and peak rate of flow required.

#### CONCLUSIONS

A theoretical investigation was conducted to determine the effects of control-surface-servo natural frequency on the dynamic performance characteristics of a supersonic canard missile configuration stabilized longitudinally by controlling the normal acceleration of the missile. As a result of this investigation, the following conclusions are reached.

Based upon a unit step command signal, 80 radians per second is a good compromise value for servo natural frequency yielding a system with high accuracy of control along with moderate servo volume of oil flow and peak rate of volume flow at all flight conditions and size factors.

The accuracy of control is roughly proportional to the size factor for all servo natural frequencies at sea level and  $M = 1.6$  and indicated an advantage in controlling smaller missiles. This argument is further strengthened by the fact that a decrease in total oil volume as well as the peak rate of volume flow necessary for control are realized for smaller missile configurations.

For a missile size factor of unity, increasing the Mach number improves the accuracy of control and decreases the total volume as well as the peak rate of volume flow, but increasing the altitude decreases the accuracy of control and increases the volume of oil flow.

The information obtained from investigations of this type may be used by the system designer in conjunction with space, accuracy of control, and economic considerations to determine the most practical automatic pilot specifications. It may be that for a specific application the additional cost and peak rate of volume flow might prohibit designing an auto-pilot with a natural frequency greater than 80 radians per second in view of the small improvement in control accuracy obtained. For other

~~CONFIDENTIAL~~

NACA RM L53G23a

configurations, a similar investigation would be necessary; however, it appears that similar results and conclusions would be obtained with this type of autopilot.

Langley Aeronautical Laboratory,  
National Advisory Committee for Aeronautics,  
Langley Field, Va., July 23, 1953.

## REFERENCES

1. Nelson, Walter C., and Passera, Anthony L.: A Theoretical Investigation of the Influence of Auxiliary Damping in Pitch on the Dynamic Characteristics of a Proportionally Controlled Supersonic Canard Missile Configuration. NACA RM L50F30, 1950.
2. Passera, Anthony L.: A Theoretical Investigation of the Influence of Autopilot Natural Frequency Upon the Dynamic Performance Characteristics of a Supersonic Canard Missile Configuration With a Pitch-Attitude Control System. NACA RM L51H02, 1951.
3. Seaberg, Ernest C., and Smith, Earl F.: Theoretical Investigation of an Automatic Control System With Primary Sensitivity to Normal Accelerations as Used To Control a Supersonic Canard Missile Configuration. NACA RM L51D23, 1951.
4. Zarovsky, Jacob, and Gardiner, Robert A.: Flight Investigation of a Roll-Stabilized Missile Configuration at Varying Angles of Attack at Mach Numbers Between 0.8 and 1.79. NACA RM L50H21, 1951.
5. Brown, Gordon S., and Campbell, Donald P.: Principles of Servomechanisms. John Wiley & Sons, Inc., 1948.
6. Chestnut, Harold, and Mayer, Robert W.: Servomechanisms and Regulating System Design. Vol. I. John Wiley & Sons, Inc., 1951.

~~CONFIDENTIAL~~

TABLE I.- AIRFRAME TRANSFER FUNCTION CONSTANTS FOR VARIOUS VALUES OF  
MACH NUMBER, ALTITUDE, AND SIZE FACTOR

$$\left[ \text{Static margin} = 0.564\bar{c} \text{ at } M = 1.60; \frac{\dot{\theta}_o(s)}{\delta} = \frac{K_m \omega_{n_m}^2 (\tau s + 1)}{s^2 + 2\zeta_m \omega_{n_m} s + \omega_{n_m}^2}; \right]$$

$$\left[ \frac{n_o}{\dot{\theta}_o}(s) = \frac{K_g}{\tau s + 1} \right]$$

Size factor	Mach number	Altitude	$K_m$	$2\zeta_m \omega_{n_m}$	$\omega_{n_m}^2$	$\tau$	$K_g$
0.4	1.6	Sea level	5.301	21.6	8243	0.089	0.967
.7	1.6	Sea level	3.030	12.3	2691	.155	.967
1.0	1.6	Sea level	2.121	8.64	1319	.222	.967
2.0	1.6	Sea level	1.064	4.32	329	.444	.967
1.0	1.2	Sea level	1.727	7.15	919	.256	.726
1.0	1.6	40,000 ft	0.456	1.84	241	1.045	.842
1.0	2.0	Sea level	2.374	9.86	1786	.187	1.210



CONFIDENTIAL

NACA RM L53G23a

TABLE II.- IDEAL INTEGRATOR AND RATE-GYRO GAIN CONSTANTS TABULATED  
 AGAINST CONTROL-SURFACE-SERVO NATURAL FREQUENCY FOR  
 VARIOUS VALUES OF SIZE FACTOR

[These values were adjusted at  $M = 1.6$  for sea-level condition.  
 $K_A$  was arbitrarily set equal to unity for all cases.]

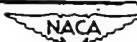
Size factor	$\omega_n$ , radians per second -							
	30		50		80		150	
	$K_r$	$K_s$	$K_r$	$K_s$	$K_r$	$K_s$	$K_r$	$K_s$
0.4	0.0251	3.09	0.0100	3.55	0.0071	3.98	0.0158	6.31
.7	.0158	3.24	.0100	3.98	.0251	5.75	.0282	6.76
1.0	.0200	5.01	.0320	6.31	.0450	7.94	.0450	8.41
2.0	.0600	6.92	.0708	7.94	.0803	8.13	.0900	8.20



CONFIDENTIAL

TABLE III.- ROOTS OF CHARACTERISTIC EQUATION OF  $n_o/n_i$  TABULATED  
 AGAINST SIZE FACTOR, MACH NUMBER, ALTITUDE,  
 AND SERVO NATURAL FREQUENCY

Size factor	Mach number	$\omega_n$	Altitude	Roots of characteristic equation of $n_o/n_i$			
0.4	1.6	30	Sea level	-23.09	-8.18 ± j 23.33	-6.07 ± j 91.03	
.4	1.6	50	Sea level	-26.34	-15.18 ± j 37.98	-7.45 ± j 91.94	
.4	1.6	80	Sea level	-27.79	-27.59 ± j 59.59	-9.30 ± j 94.30	
.4	1.6	150	Sea level	-52.4	-37.98 ± j 69.74	-21.60 ± j 132.96	
.7	1.6	30	Sea level	-13.47	-10.13 ± j 22.58	-4.30 ± j 52.60	
.7	1.6	50	Sea level	-15.36	-16.68 ± j 39.11	-6.78 ± j 52.71	
.7	1.6	80	Sea level	-25.76	-22.49 ± j 40.53	-10.77 ± j 71.60	
.7	1.6	150	Sea level	-28.34	-16.66 ± j 46.32	-50.32 ± j 122.19	
1.0	1.6	30	Sea level	-14.59	-8.12 ± j 23.00	-3.89 ± j 37.27	
1.0	1.6	50	Sea level	-19.68	-13.03 ± j 29.13	-6.45 ± j 45.68	
1.0	1.6	80	Sea level	-27.54	-12.08 ± j 29.92	-18.46 ± j 66.72	
1.0	1.6	150	Sea level	-24.8	-9.49 ± j 31.97	-57.39 ± j 123.29	
2.0	1.6	30	Sea level	-10.21	-7.38 ± j 24.75	-4.66 ± j 16.92	
2.0	1.6	50	Sea level	-11.25	-17.68 ± j 40.95	-3.85 ± j 16.82	
2.0	1.6	80	Sea level	-11.12	-32.44 ± j 66.17	-4.16 ± j 16.54	
2.0	1.6	150	Sea level	-10.38	-68.12 ± j 126.5	-3.84 ± j 16.60	
1.0	1.2	30	Sea level	-8.13	-11.00 ± j 22.58	-3.51 ± j 31.63	
1.0	1.2	50	Sea level	-10.17	-10.29 ± j 30.63	-13.19 ± j 39.21	
1.0	1.2	80	Sea level	-13.23	-9.69 ± j 28.24	-27.26 ± j 64.97	
1.0	1.2	150	Sea level	-12.89	-7.79 ± j 28.18	-64.32 ± j 125.00	
1.0	1.6	30	40,000 ft	-2.08	-13.71 ± j 25.28	-1.17 ± j 15.54	
1.0	1.6	50	40,000 ft	-2.59	-22.97 ± j 42.22	-1.65 ± j 15.52	
1.0	1.6	80	40,000 ft	-3.28	-37.19 ± j 67.80	-2.08 ± j 15.34	
1.0	1.6	150	40,000 ft	-3.41	-72.30 ± j 128.43	-1.91 ± j 15.25	
1.0	2.0	30	Sea level	-19.68	-5.37 ± j 24.64	-4.72 ± j 42.72	
1.0	2.0	50	Sea level	-28.04	-11.42 ± j 31.65	-4.49 ± j 50.29	
1.0	2.0	80	Sea level	-40.26	-11.82 ± j 33.64	-12.97 ± j 70.17	
1.0	2.0	150	Sea level	-37.61	-9.79 ± j 36.91	-51.33 ± j 122.73	



CONFIDENTIAL

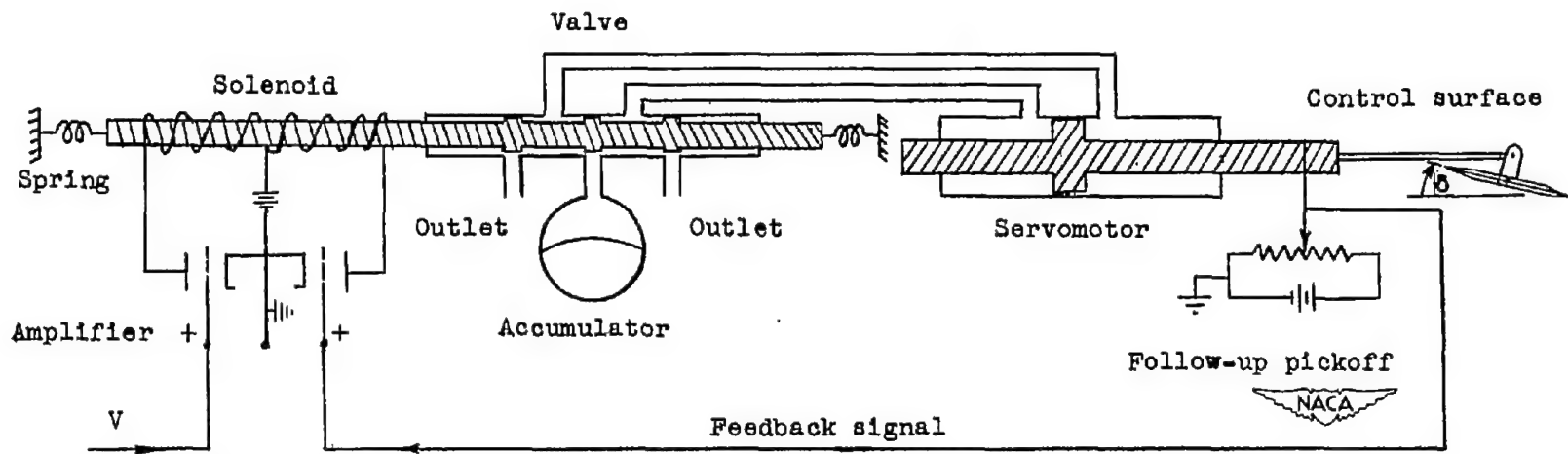


Figure 1.- Schematic diagram of a possible control-surface servo having a second-order characteristic equation.

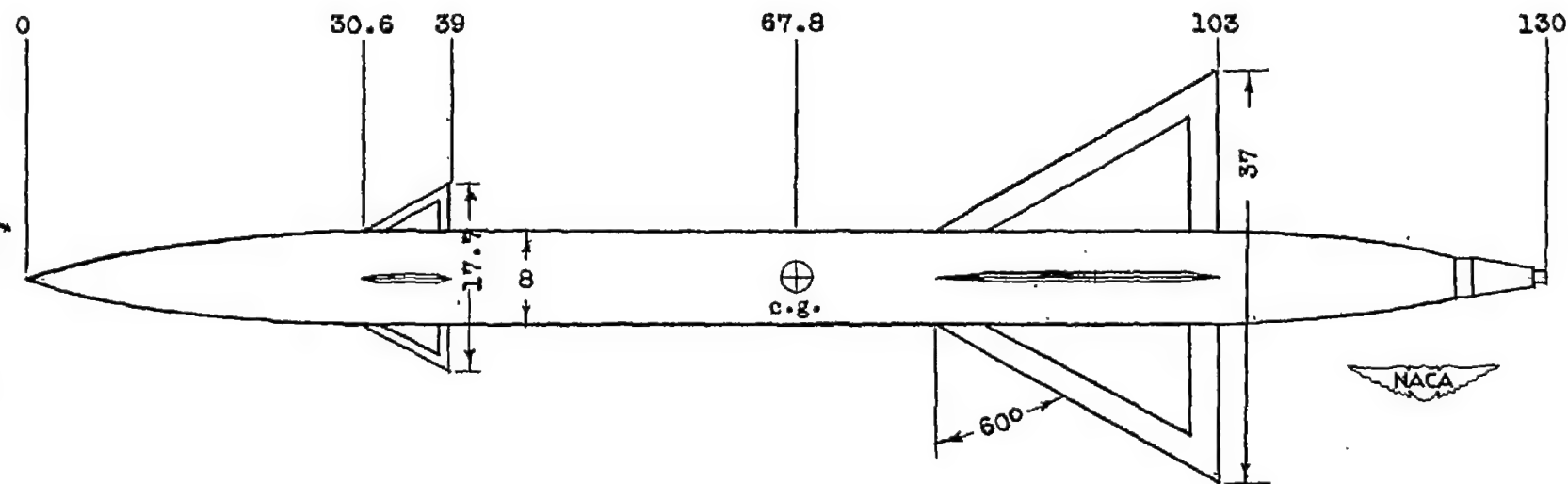


Figure 2-- Sketch of missile configuration showing dimensions of model having a size factor = 1.0. All dimensions are in inches.

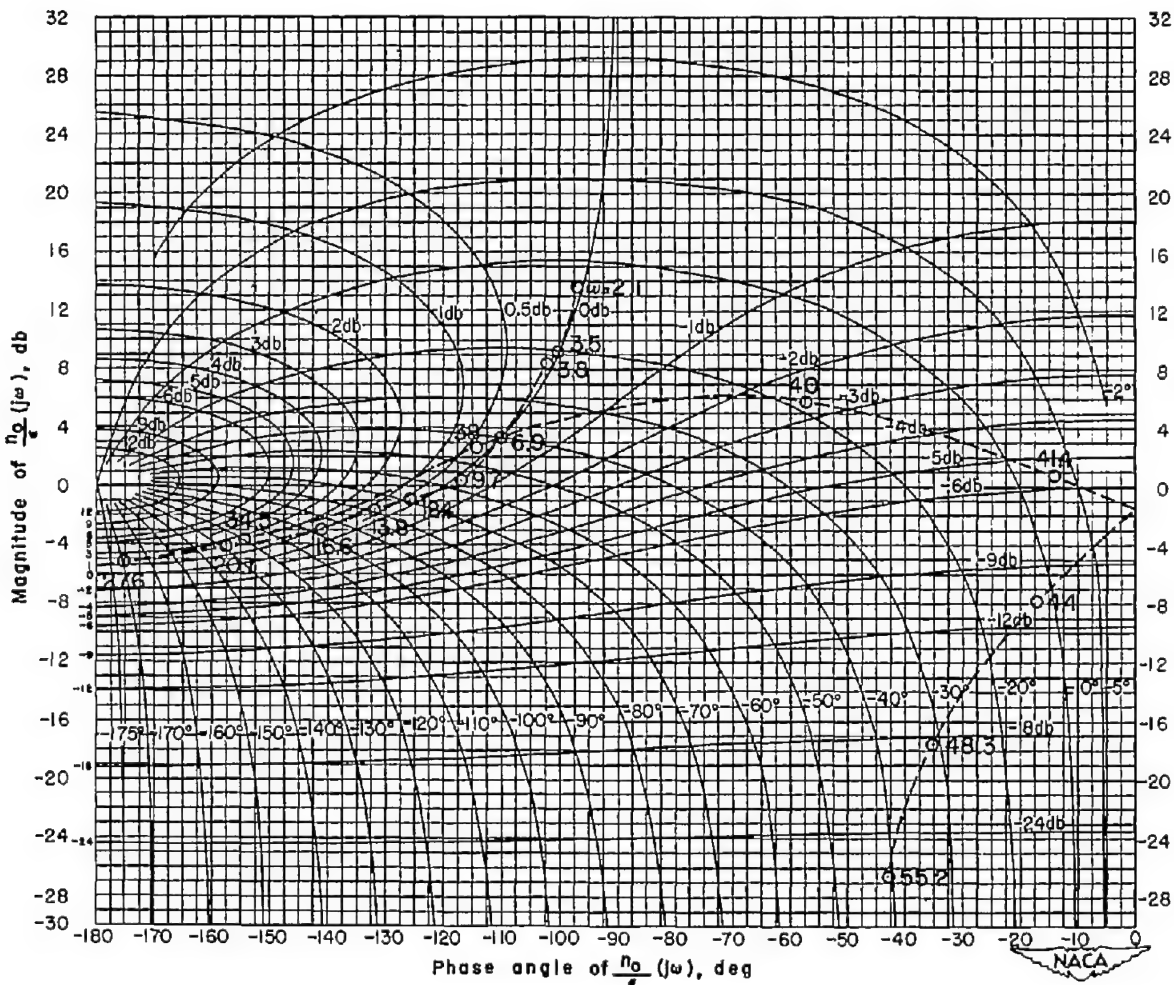
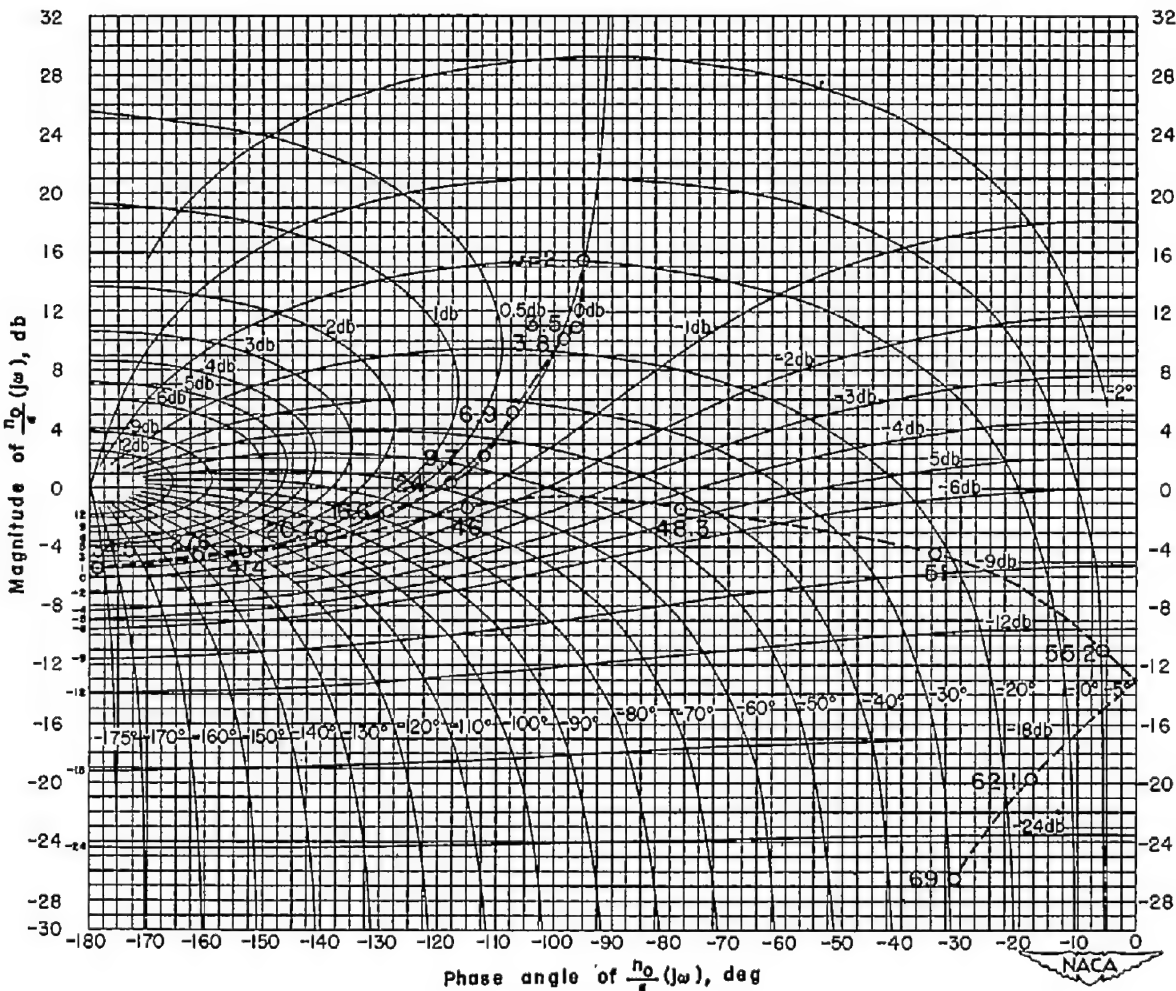


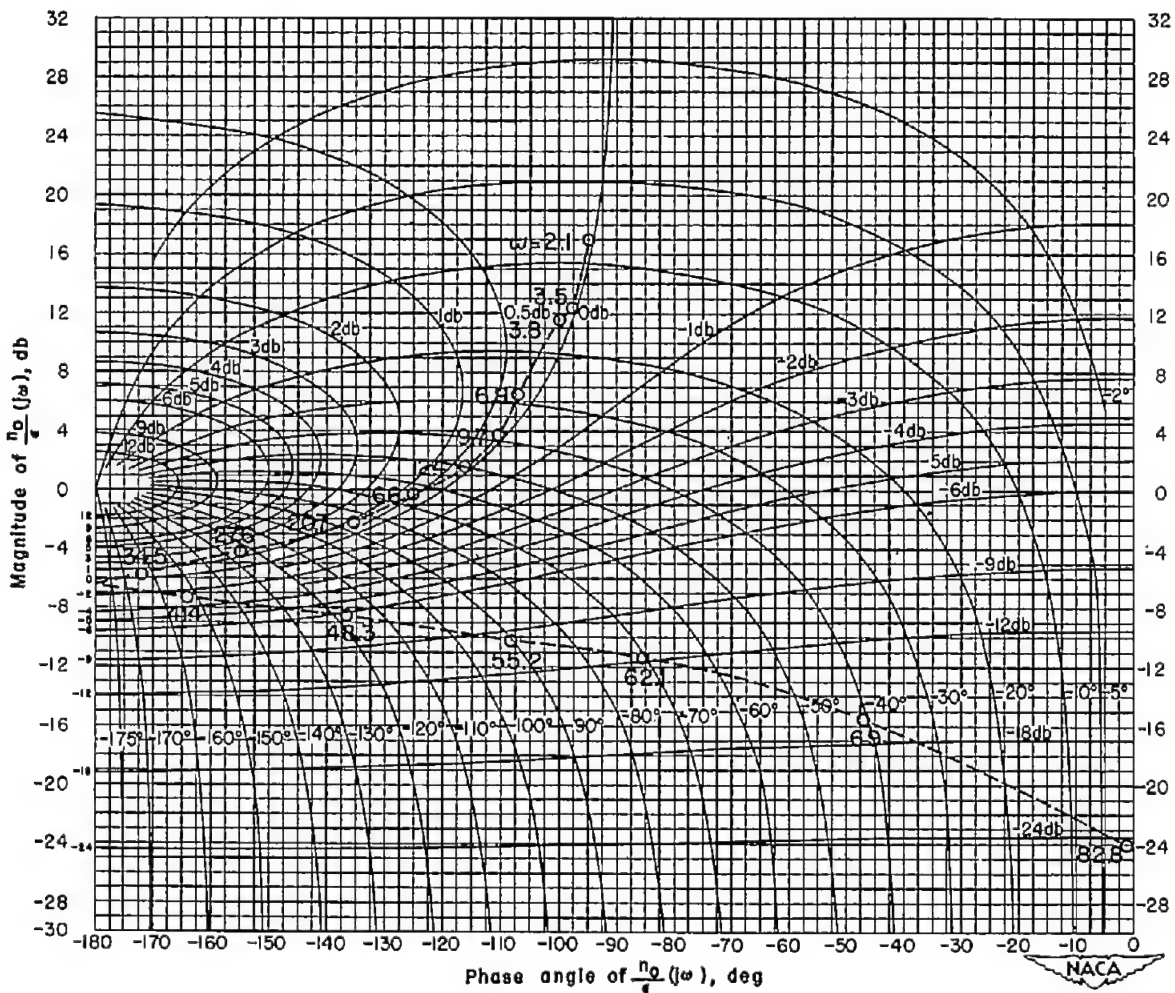
Figure 3.- Nichols chart showing system frequency responses for the final gain adjustments.  $M = 1.6$ ; sea level; size factor, 1.0.

CONFIDENTIAL



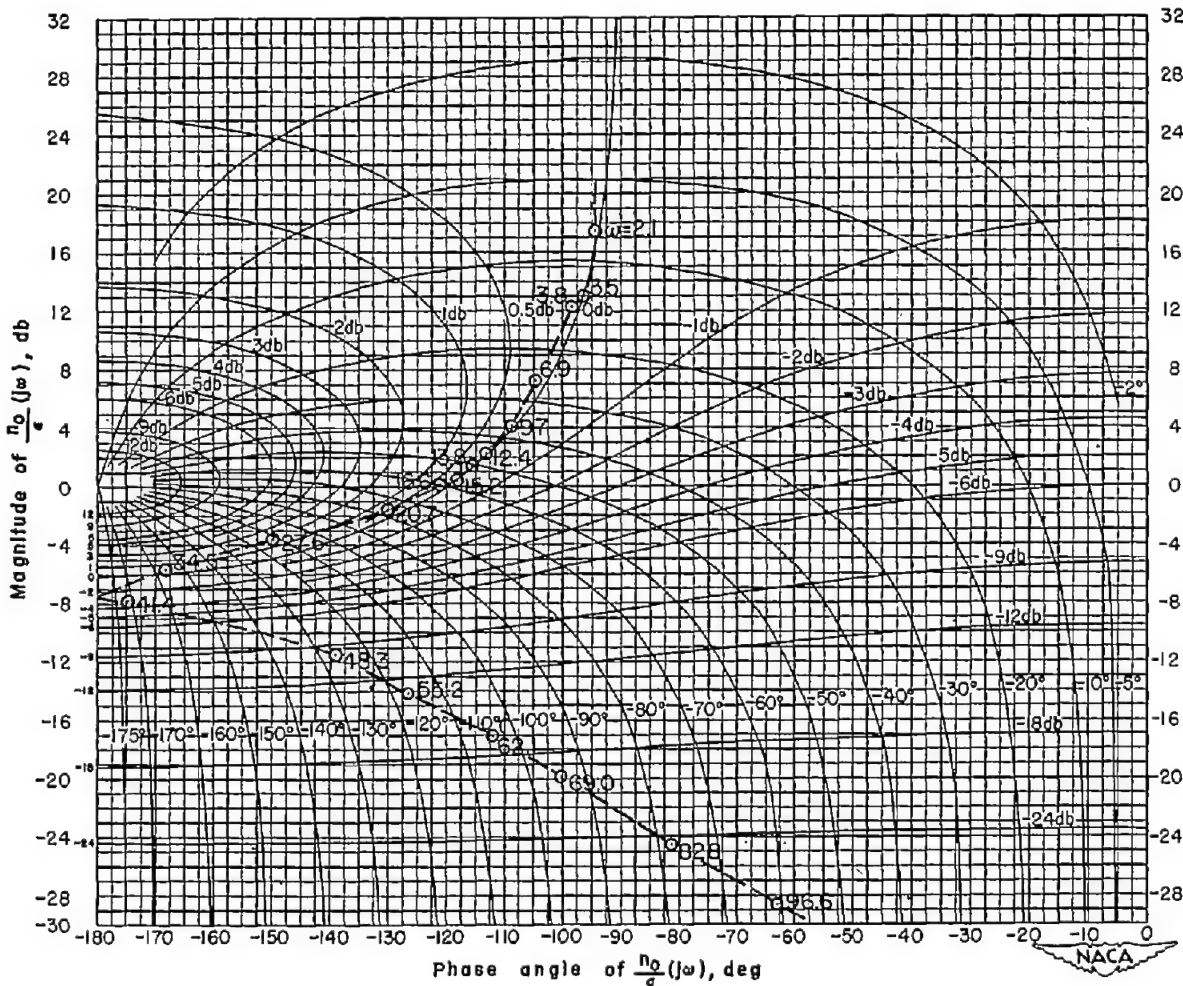
(b)  $\omega_n = 50$ ;  $K_T = 0.032$ ;  $K_B = 6.31$ .

Figure 3.- Continued.



(c)  $\omega_n = 80$ ;  $K_r = 0.045$ ;  $K_B = 7.94$ .

Figure 3.- Continued.

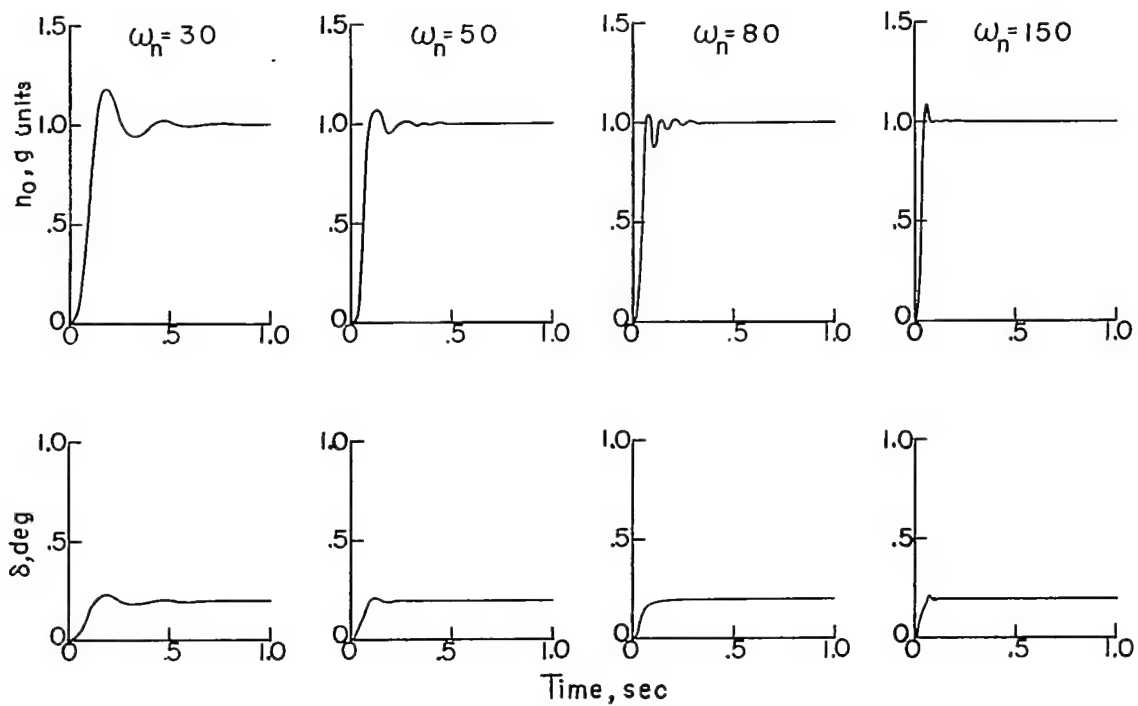


$$(a) \quad \omega_n = 150; \quad K_T = 0.045; \quad K_S = 8.41.$$

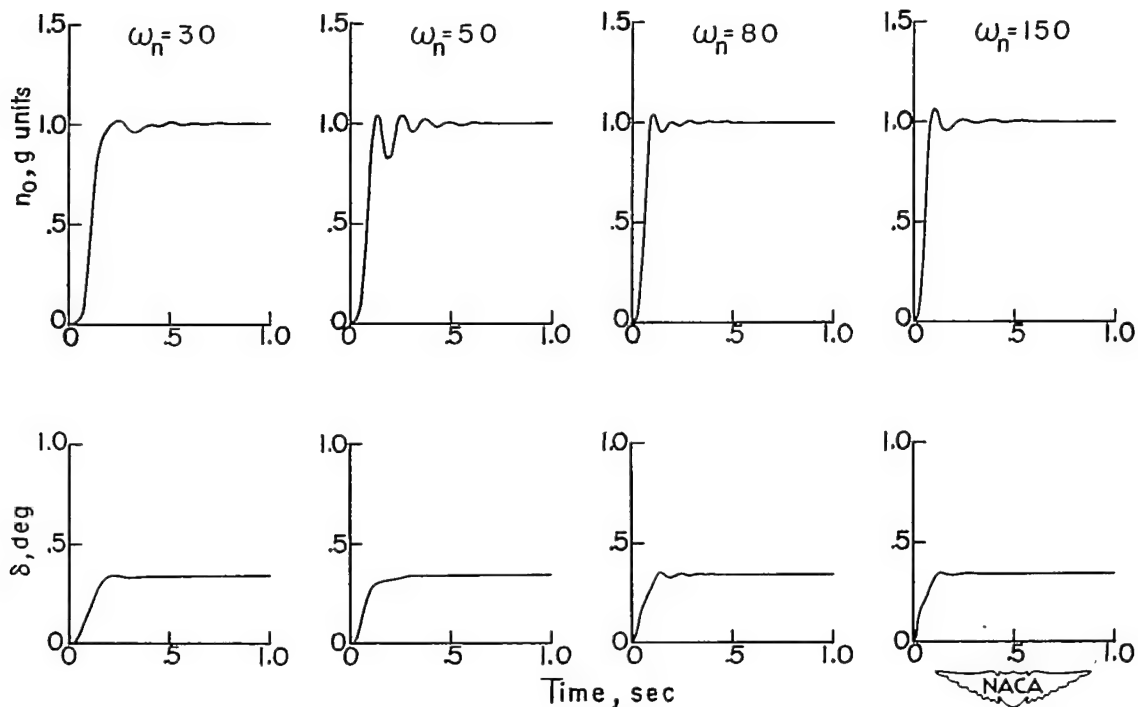
Figure 3.- Concluded.

~~CONFIDENTIAL~~

NACA RM L53G23a



(a) Size factor = 0.4.

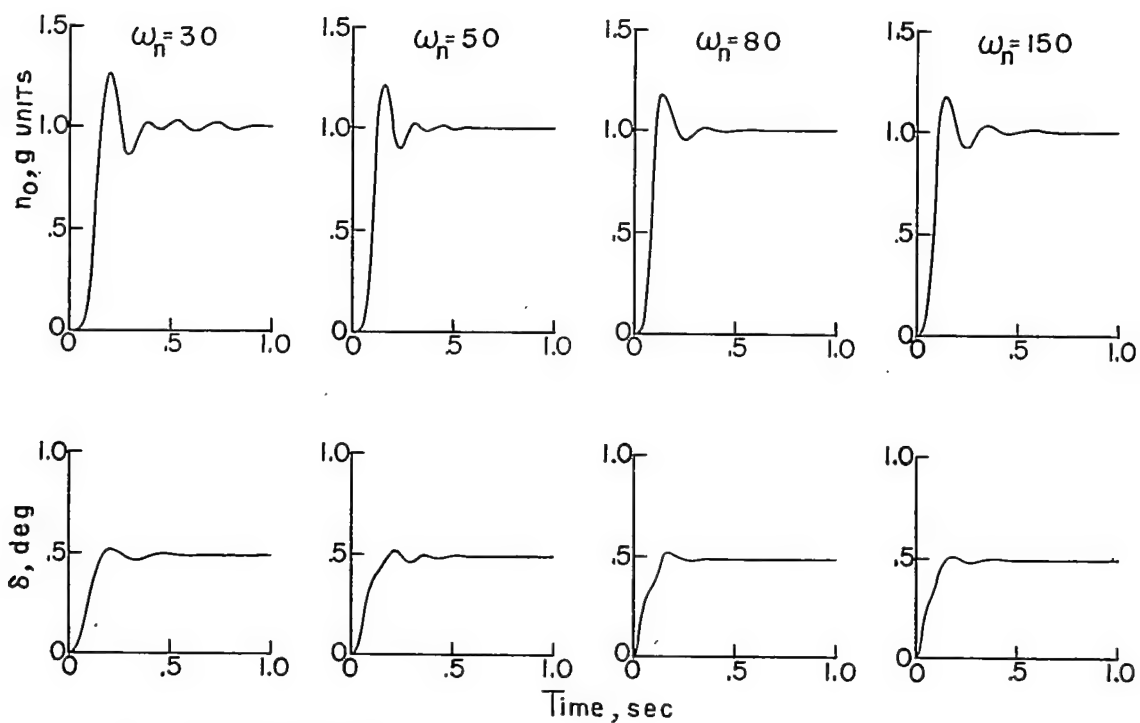


(b) Size factor = 0.7.

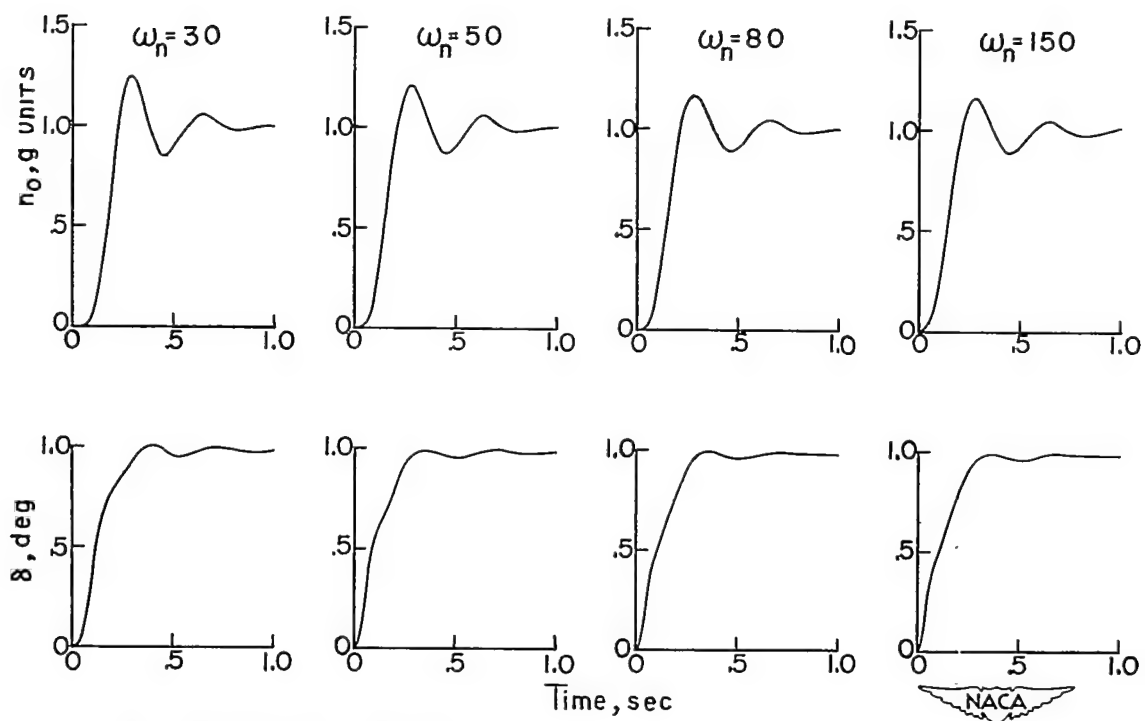
Figure 4.- Transient responses  $n_o(t)$  and  $\delta(t)$  of the control system to a unit step acceleration input of 1g.  $M = 1.6$  at sea level.

~~CONFIDENTIAL~~

NACA



(c) Size factor = 1.0.



(d) Size factor = 2.0.

Figure 4.- Concluded.

CONFIDENTIAL

NACA RM L53G23a

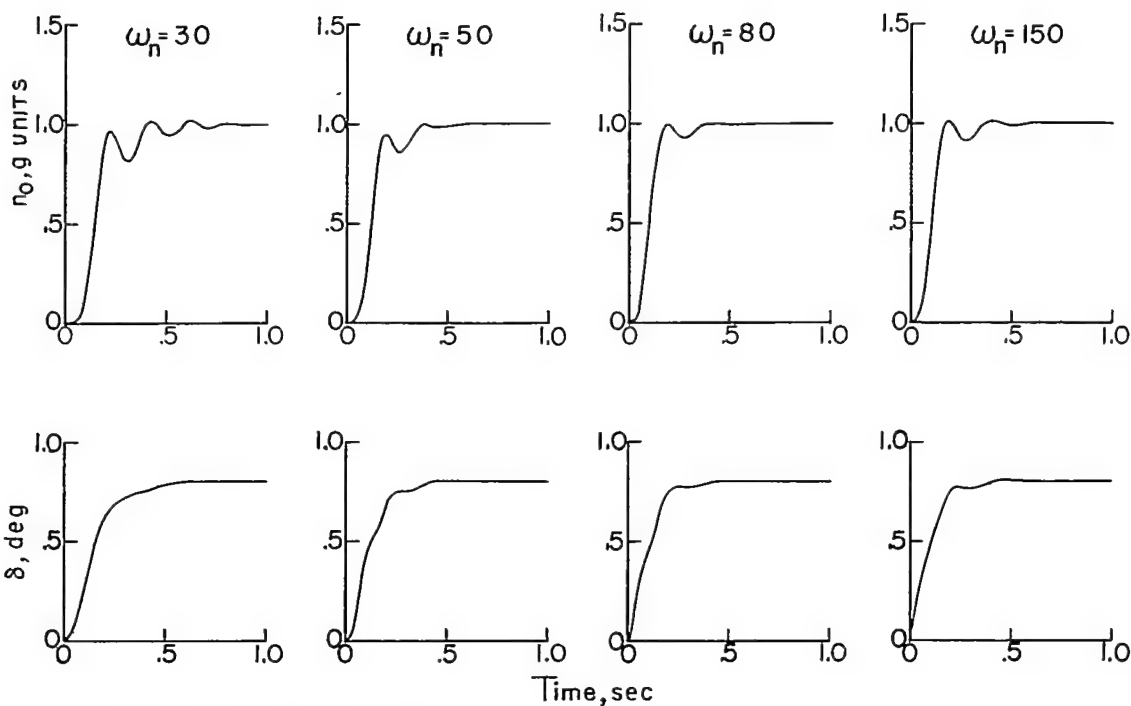
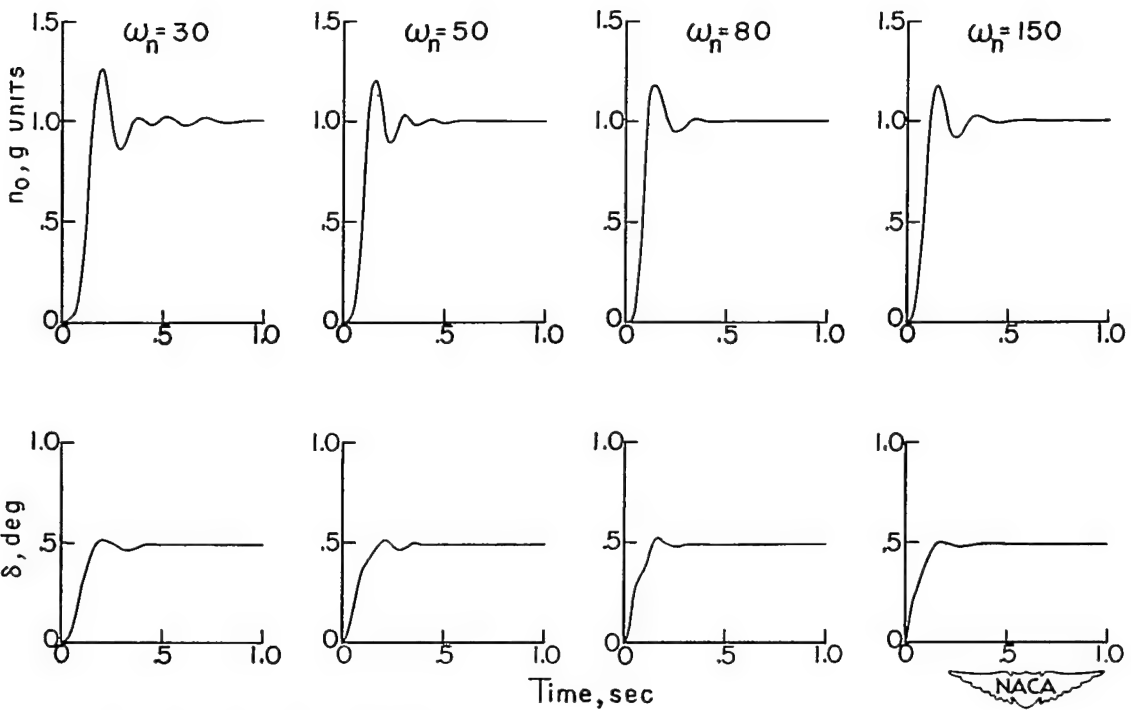
(a)  $M=1.2$ ; sea level.(b)  $M=1.6$ ; sea level.

Figure 5.- Transient responses  $n_0(t)$  and  $\delta(t)$  of the control system to a unit step acceleration input of 1g. Size factor, 1.0.

CONFIDENTIAL

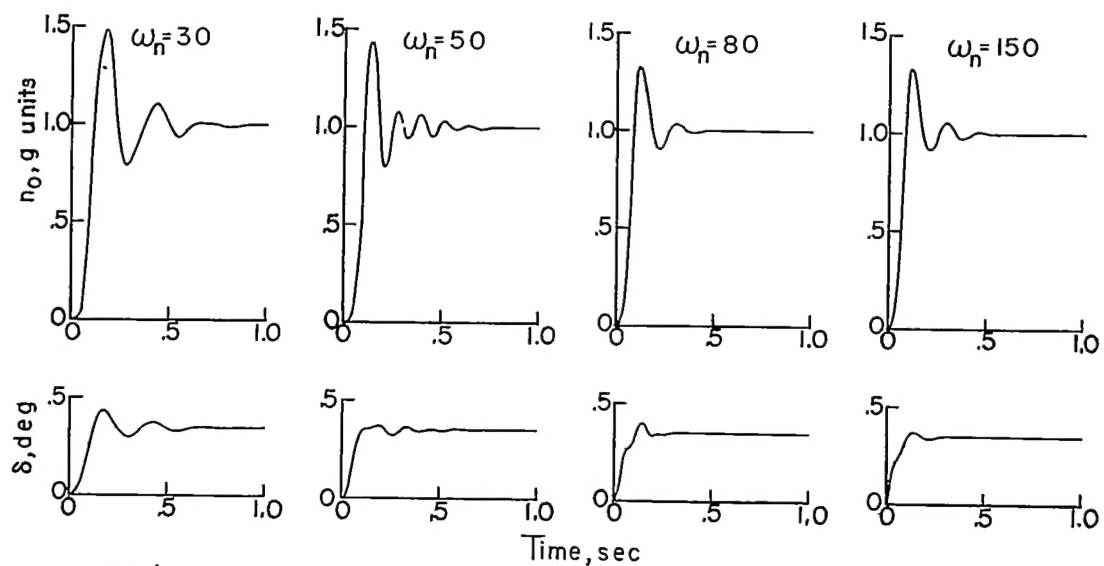
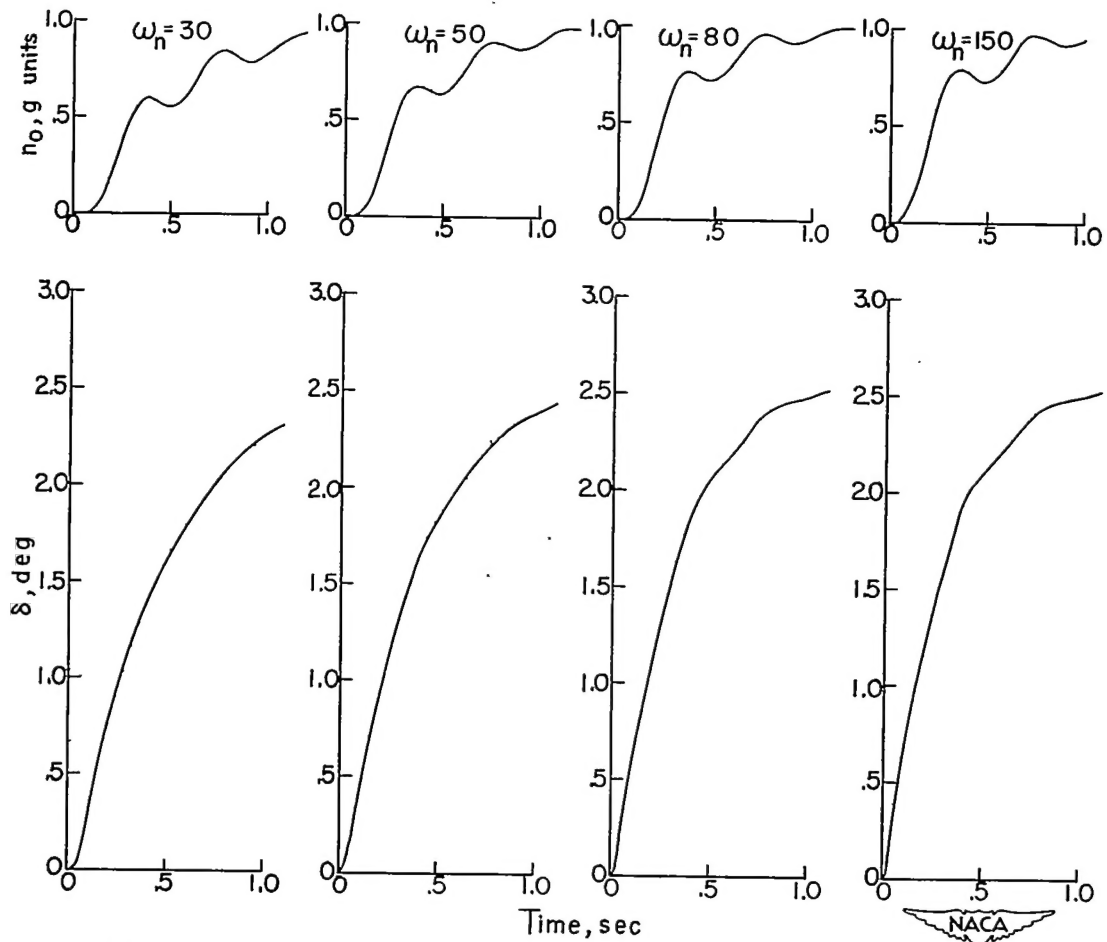
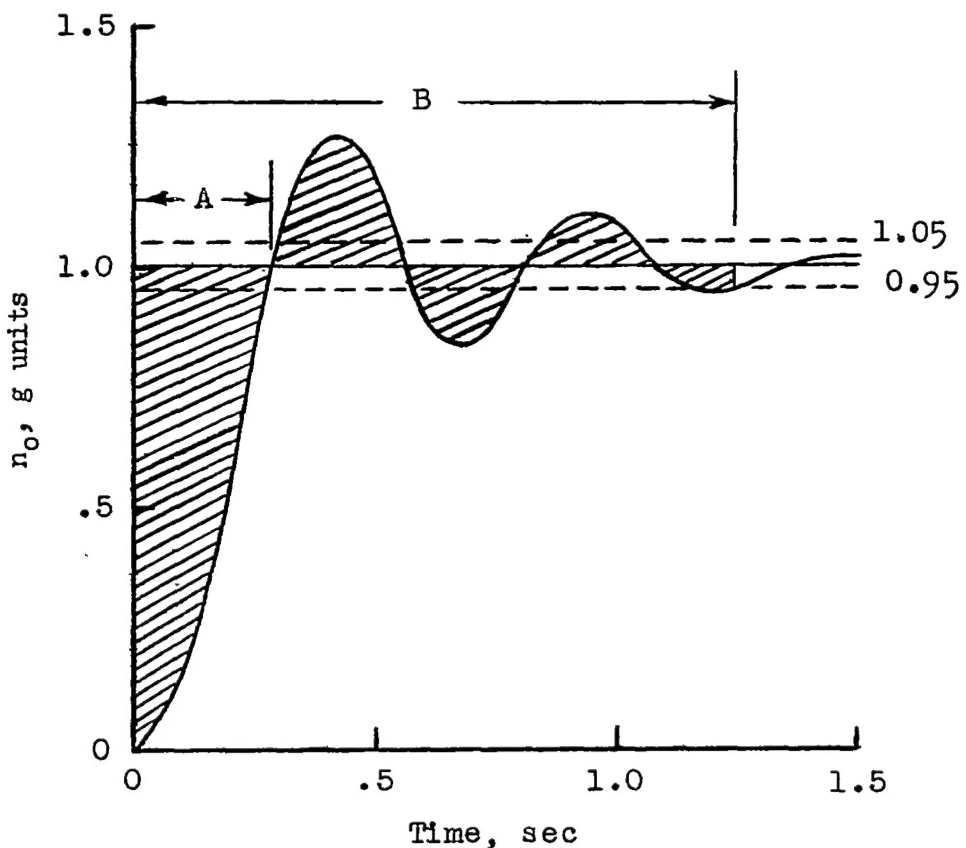
(c)  $M = 2.0$ ; sea level.(d)  $M = 1.6$ ; 40,000 ft.

Figure 5.- Concluded.

CONFIDENTIAL

NACA RM L53G23a



$$\text{Shaded area} - \int |\epsilon(t)| dt$$

A — Rise time  
 B — Response time



Figure 6.- Representative output transient response illustrating the normal-acceleration transient characteristics.

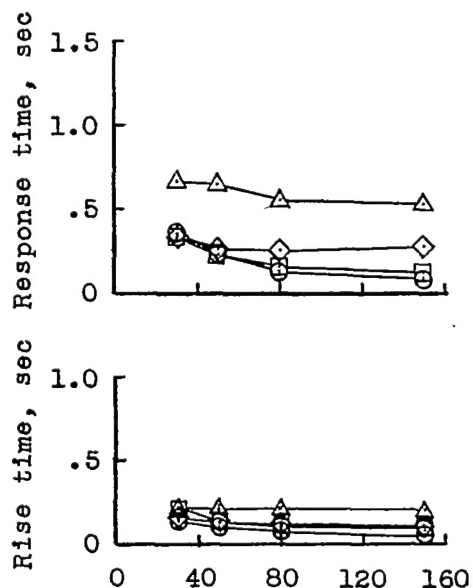
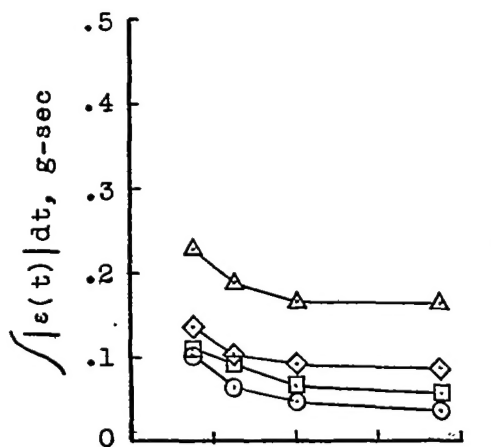
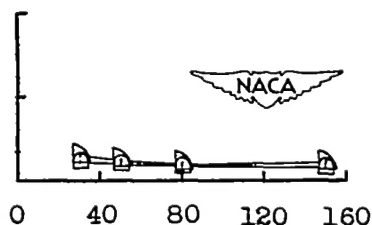
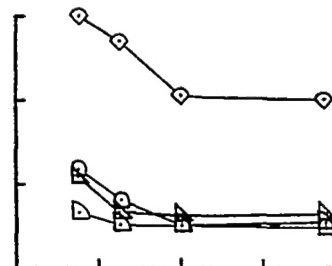
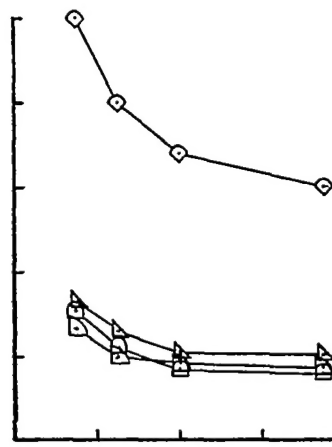
CONFIDENTIAL

$M = 1.6$ ; Sea level

- Size factor = 0.4
- Size factor = 0.7
- ◊ Size factor = 1.0
- △ Size factor = 2.0

Size factor = 1.0

- ▷ M = 1.2; Sea level
- ▷ M = 1.6; Sea level
- ▷ M = 2.0; Sea level
- ◊ M = 1.6; 40,000 feet

Control-surface-servo natural frequency,  $\omega_n$ , radians/sec

NACA

Figure 7.- Normal-acceleration transient characteristics,  $\int |\epsilon(t)| dt$ , rise time, and response time, in response to a step input  $n_i(t)$  plotted against control-surface-servo natural frequency. Static margin equals 0.564 at  $M = 1.6$ .

CONFIDENTIAL

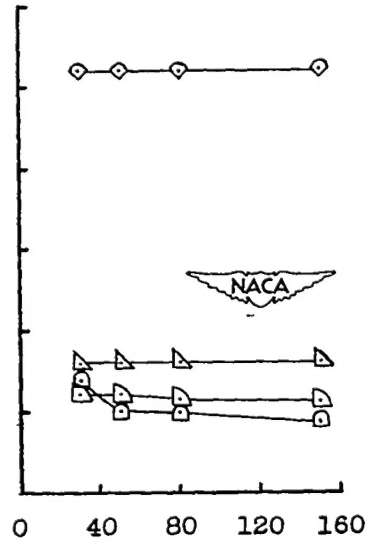
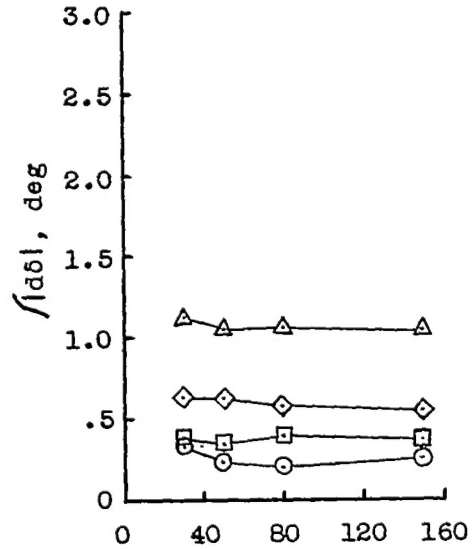
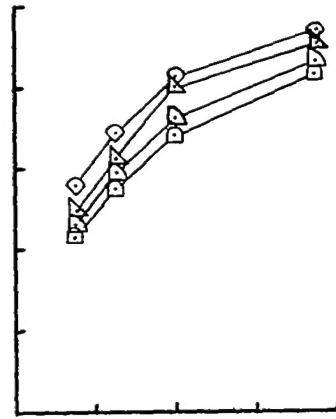
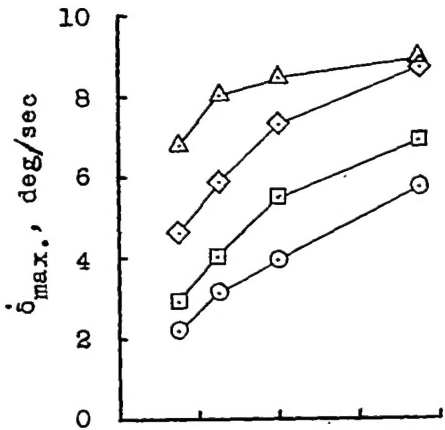
CONFIDENTIAL

 $M = 1.6$ ; Sea level

- Size factor = 0.4
- Size factor = 0.7
- ◇ Size factor = 1.0
- △ Size factor = 2.0

Size factor = 1.0

- ▽ M = 1.2; Sea level
- M = 1.6; Sea level
- M = 2.0; Sea level
- ◇ M = 1.6; 40,000 feet



Control-surface-servo natural frequency,  $\omega_n$ , radians/sec

Figure 8.- Control-surface-servo characteristics,  $\dot{\delta}_{\max}$  and  $\int |d\delta|$ ,

in response to a step input  $n_1(t)$  plotted against control-surface-servo natural frequency. Static margin equals  $0.564c$  at  $M = 1.6$ .

CONFIDENTIAL